A Sparse Sampling Method in the Two-dimensional Spatial Domain for Sheared-beam Imaging Receiving System

Minglai Chen[a,b,c], Caiwen Ma*[a,b,c], Xiujuan Luo[a,b,c], Hui Liu[a,b,c], Yu Zhang[a,c], Zelin Yue[a,b], Jing Zhao[a,b]

[a]Xi'an Institute of Optics and Precision Mechanics, Chinese Academy of Sciences, Xi'an 710119, China

[b]University of Chinese Academy of Sciences, Beijing 100049, China

[c]Key Laboratory of Space Precision Measurement Technology, Chinese Academy of Sciences, Xi'an 710119, China

ABSTRACT

In the imaging of low-orbit moving objects, the number of detector elements in the traditional sheared-beam imaging (SBI) system is too great, which seriously restrict the application of SBI. In this paper, the detector array is sparse in two dimensions. We propose a two-dimensional sparse sampling imaging method, which emits a two-dimensional coherent laser array, carries more spectral information of the target at a time and receives speckle echo signals by a two-dimensional sparse detector array for computational imaging. This method can reduce the number of detector elements many times. Firstly, the principle of two-dimensional sparse sampling with SBI detector array is deduced theoretically. Secondly, a two-dimensional spatial sparse reconstruction algorithm is investigated. The target amplitude product and phase difference carried by each detector array element is estimated using discrete Fourier transform, then the target amplitude product and phase difference of all detector array elements are matched respectively to form a complete target amplitude product surface and phase difference surface. The formulas of phase recovery and amplitude demodulation are derived. Finally, the validity and feasibility of the proposed method are verified by simulation. Compared with the traditional three-beam method, when the number of lasers in emission array is $M \times N$, the number of detector elements is reduced to $1/(M\text{-}1)/(N\text{-}1)$ of the original without loss of imaging resolution.

Keywords: Shear-beam imaging, computational imaging, two-dimensional spatial domain, sparse sampling

1. INTRODUCTION

The absorption, refraction, scattering and jitter of light in the atmosphere seriously affect the effectiveness of ground-based optical imaging of space targets[1]. Traditional passive imaging methods often overcome the effects of atmospheric turbulence with complex adaptive optical systems. SBI is a active imaging technique, which can break through the aperture of the telescope to the limit of imaging resolution and enables high-resolution imaging of remote targets through atmospheric turbulence[2-14]. SBI system illuminates a target using three laser beams with slightly different frequencies arranged as an "L" in the emission plane, and receives echo signal by a detector array for computational imaging[4]. Using this method of small emission shear length, frequency modulation, and phase difference of the light pupil, the effects of atmospheric turbulence on imaging can be effeftively overcome. In the absence of adaptive optics and imaging lenses, target images approaching diffraction limits can be acquired[2]. SBI technology has the advantage of quasi-real-time imaging, and has a broad prospect of application in remote moving target imaging[4].

The SBI system uses a discrete detector array to sample the echo signal. In the traditional three-beam imaging system, only the detector spacing is consistent with the emission shear length can the image be reconstructed by the image reconstruction algorithm[14]. In the imaging of low-orbit targets, however, if a large equivalent aperture receiving system is used to achieve high resolution imaging, as the number of detector elements becomes extremely large[10], the cost of the detector array becomes very high, and the implementation is very challenging. Therefore, it is very necessary

*cwma@opt.ac.cn

SPIE-CLP Conference on Advanced Photonics 2022, edited by Xu Liu, Anatoly Zayats, Xiaocong Yuan, Proc. of SPIE Vol. 12601, 126010M
 · 0277-786X · doi: 10.1117/12.2666901

to sparse the detector array.

The literature [15] proposed a one dimensional sparse sampling imaging method for the SBI system, where five laser beams are emitted at once and the number of detector elements in the detector array can be sparse as much as half of the traditional three-beam imaging system. This paper proposes a two-dimensional sparse sampling imaging method, which extends the one-dimensional sparsity of the detector array to two-dimensional sparsity, and further reduces the number of detector elements.

2. IMAGING PRINCIPLE AND METHOD

2.1 The principle of sparse sampling in two-dimensional spatial domain

This paper presents a sparse sampling method in two-dimensional spatial domain for SBI receiving system, and the schmetic diagram of the imaging system is shown in Figure 1. The coherent laser beams in a two-dimensional array are emitted to illumate the target, and the echo signals are received via detector array which has been sparse. Assuming that the number of coherent lasers is $M \times N$, the transverse and longitudinal emission shear length is s_x, s_y, respectively. The transverse detector spacing is $(M-1)s_x$, and the longitudinal detector spacing is $(N-1)s_y$. When the number of detector elements in receiving array of the proposed imaging system is only $\frac{1}{(M-1)(N-1)}$ of the traditional three-beam system, the both imaging system can achieve the same imaging resolution.

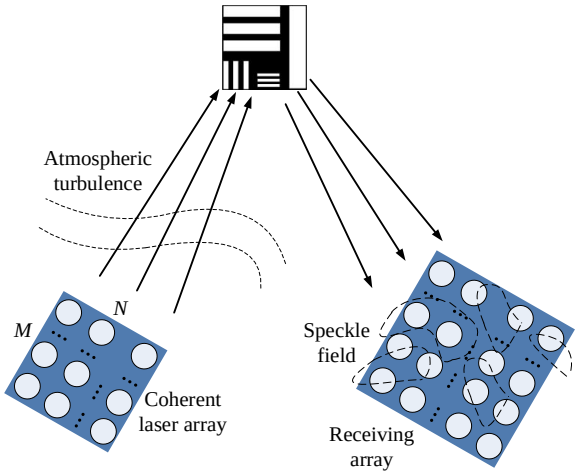

Figure 1. Schmetic diagram of the two-dimensional sparse sampling imaging system

The optical field expression at any point (x', y') on the surface of the target is[15]:

$$U(x', y', t) = \sum_{i=0}^{M-1} \sum_{j=0}^{N-1} E_{ij} \exp[\mathrm{i}(\mathbf{k}_{ij}\mathbf{r}_{ij} - \omega_{ij} t)], \tag{1}$$

where E_{ij}, ω_{ij} is the amplitude and angular frequency of the (i, j)th beam of light respectively. The laser frequency is set according to Golomb ruler[16]. $\mathbf{k}_{ij}$ is the wave number. $\mathbf{r}_{ij}$ is the displacement vector of the laser transmit aperture and the target surface. The scalar values of $\mathbf{r}_{ij}$ is expressed as follows:

$$r_{ij} = \sqrt{R^2 + (x' - i \cdot s_x)^2 + (y' - j \cdot s_y)^2}, \tag{2}$$

where R is the imaging distance.

Since $R^2 \gg x'^2 + y'^2, R^2 \gg s_x^2 + s_y^2$, the following expression is derived:

$$r_{ij} \approx R + \frac{x'^2 + y'^2}{2R} - \frac{i \cdot s_x}{R} x' - \frac{j \cdot s_y}{R} y' . \tag{3}$$

Substituting equation (3) into equation (1) gives

$$\begin{aligned} U(x', y', t) &= \sum_{i=0}^{M-1} \sum_{j=0}^{N-1} E_{ij} \exp[\mathrm{i}(\mathbf{k}_{ij} \mathbf{r}_{ij} - \omega_{ij} t)] \\ &= \sum_{i=0}^{M-1} \sum_{j=0}^{N-1} E_{ij} \exp(-\mathrm{i}\,\omega_{ij} t) \exp\left[-\mathrm{i} \left(2\pi \frac{i \cdot s_x}{\lambda R} x' \right) \right] \exp\left[-\mathrm{i} \left(2\pi \frac{j \cdot s_y}{\lambda R} y' \right) \right]. \end{aligned} \tag{4}$$

According to the Fraunhofer diffraction principle, the scattering field formed by the laser on the plane of the detector array through a diffuse reflection target is as follows:

$$\begin{aligned} A(x, y, t) &= \iint o(x', y') U(x', y', t) \exp\left(-\mathrm{i} \cdot 2\pi u x'\right) \exp\left(-\mathrm{i} \cdot 2\pi v y'\right) dx' dy' \\ &= \sum_{i=0}^{M-1} \sum_{j=0}^{N-1} E_{ij} \exp(-\mathrm{i}\,\omega_{ij} t) \iint o(x', y') \exp\left[-\mathrm{i}\, 2\pi (u + i \cdot s_x / (\lambda R)) x'\right] \\ &\quad \times \exp\left[-\mathrm{i} \cdot 2\pi (v + j \cdot s_y / (\lambda R)) y'\right] dx' dy' \\ &= \sum_{i=0}^{M-1} \sum_{j=0}^{N-1} E_{ij} \exp\left(-\mathrm{i}\,\omega_{ij} t\right) O\left(u + i \cdot s_x / (\lambda R), v + j \cdot s_y / (\lambda R)\right) \\ &= \sum_{i=0}^{M-1} \sum_{j=0}^{N-1} E_{ij} \exp\left(-\mathrm{i}\,\omega_{ij} t\right) A_0\left(u + i \cdot s_x / (\lambda R), v + j \cdot s_y / (\lambda R)\right) \\ &\quad \times \exp\left[\mathrm{i}\, \phi\left(u + i \cdot s_x / (\lambda R), v + j \cdot s_y / (\lambda R)\right)\right] \\ &= \sum_{i=0}^{M-1} \sum_{j=0}^{N-1} E_{ij} \exp\left(-\mathrm{i}\,\omega_{ij} t\right) A_{ij} \exp\left(\mathrm{i}\,\phi_{ij}\right) \end{aligned} \tag{5}$$

where $o(x', y')$ is a reflectivity function of the target. $u = x/(\lambda R)$, $v = y/(\lambda R)$. λ is the laser wavelength. $O(u, v)$ is the target spectrum, $A_0(u, v)$ is the wavefront amplitude, $\phi(u, v)$ is the wavefront phase. $A_{ij} \triangleq A_0\left(u + i \cdot s_x / (\lambda R), v + j \cdot s_y / (\lambda R)\right)$, $\phi_{ij} \triangleq \phi\left(u + i \cdot s_x / (\lambda R), v + j \cdot s_y / (\lambda R)\right)$.

The beat-frequency signal intensity distribution due to speckle interference is as follows[14]:

$$I(x, y, t) = \left| A(x, y, t) \right|^2 = \sum_{i=0}^{M-1} \sum_{j=0}^{N-1} E_{ij}^2 A_{ij}^2 + 2 \sum_{i=0}^{M-1} \sum_{j=0}^{N-1} \sum_{\substack{k=0 \\ i<k \text{ or } j<l}}^{M-1} \sum_{l=0}^{N-1} E_{ij} E_{kl} A_{ij} A_{kl} \cos(\Delta\omega_{ijkl} t + \Delta\phi_{ijkl}) , \tag{6}$$

where $\Delta\omega_{ijkl} = \omega_{kl} - \omega_{ij}$, $\Delta\phi_{ijkl} = \phi_{ij} - \phi_{kl}$.

The time domain echo signal (6) contains the amplitude $A_0(x, y)$ and phase $\phi(x, y)$ of the target. Because of the increase in the number of emitted lasers, the echo signal carries a great deal of phase difference information of the target, which is why the detector elements can be sparse to $\frac{1}{(M-1)(N-1)}$ of the original.

2.2 Two-dimensional spatial sparse reconstruction algorithm

The echo signal (6) is sampling using a two-dimensional discrete detector array after it has been sparse. Assuming that the number of detector elements is $\mathrm{N}_x \times \mathrm{N}_y$, the two-dimensional spatial coordinates of the detector elements are as follows:

$$\begin{aligned} x_p &= \left(p - \mathrm{N}_x / 2\right)(M-1) s_x, \\ y_q &= \left(q - \mathrm{N}_y / 2\right)(N-1) s_y, \end{aligned} \tag{7}$$

where p,q represents the serial number of the detector array, $p=1,\cdots,\mathrm{N}_x, q=1,\cdots,\mathrm{N}_y$. The time domain echo signals of the detector array are:

$$I(x_p,y_q,t)=\sum_{i=0}^{M-1}\sum_{j=0}^{N-1}E_{ij}^2A_{ij}^2+2\sum_{i=0}^{M-1}\sum_{j=0}^{N-1}\sum_{\substack{k=0\\ i<k\ or\ j<l}}^{M-1}\sum_{l=0}^{N-1}E_{ij}E_{kl}A_{ij}A_{kl}\cos(\Delta\omega_{ijkl}t+\Delta\phi_{ijkl}), \tag{8}$$

where $u=x_p/(\lambda R), v=y_q/(\lambda R)$.

Define $P=(p-1)M+1, Q=(q-1)N+1$. According to the above formula, the discrete Fourier transform is used to extract the phase difference

$$\begin{aligned}S^x_{P+i,Q+j}&=\phi\left(u+is_x/(\lambda R),v+js_y/(\lambda R)\right)-\phi\left(u+(i+1)s_x/(\lambda R),v+js_y/(\lambda R)\right)\\ S^y_{P+i,Q+j}&=\phi\left(u+is_x/(\lambda R),v+js_y/(\lambda R)\right)-\phi\left(u+is_x/(\lambda R),v+(j+1)s_y/(\lambda R)\right)\\ &\qquad i=0,1,\cdots,M-1,\ j=0,1,\cdots,N-1\end{aligned} \tag{9}$$

and the amplitude product

$$\begin{aligned}M^x_{P+i,Q+j}&=E_{i,j}E_{i+1,j}A_0\left(u+is_x/(\lambda R),v+js_y/(\lambda R)\right)A_0\left(u+(i+1)s_x/(\lambda R),v+js_y/(\lambda R)\right)\\ M^y_{P+i,Q+j}&=E_{i,j}E_{i,j+1}A_0\left(u+is_x/(\lambda R),v+js_y/(\lambda R)\right)A_0\left(u+is_x/(\lambda R),v+(j+1)s_y/(\lambda R)\right)\\ M^{xy}_{P+i,Q+j}&=E_{i+1,j}E_{i,j+1}A_0\left(u+(i+1)s_x/(\lambda R),v+js_y/(\lambda R)\right)A_0\left(u+is_x/(\lambda R),v+(j+1)s_y/(\lambda R)\right)\\ &\qquad i=0,1,\cdots,M-1,\ j=0,1,\cdots,N-1,\end{aligned} \tag{10}$$

at the corresponding frequency[17].

The target amplitude spectrum A_0 is obtained by means of algebraic operation of amplitude product (10):

$$A_0\left(u+is_x/(\lambda R),v+js_y/(\lambda R)\right)=\frac{\sqrt{M^x_{P+i,Q+j}\cdot M^y_{P+i,Q+j}/M^{xy}_{P+i,Q+j}}}{E_{i,j}}. \tag{11}$$

where $u=x_P/(\lambda R), v=y_Q/(\lambda R)$.

The target phase spectrum is derived in what follows. Redefining

$$x_{i'}=(i'-m/2)S_x,\quad i'=1,2,\cdots,m$$

$$y_{j'}=(j'-n/2)S_y,\quad j'=1,2,\cdots,n$$

where $m=M(\mathrm{N}_x-1)+1,\ n=N(\mathrm{N}_y-1)+1.$

According to equation (9), the phase difference of all the detector elements is matched and then the following phase difference matrix is derived:

$$\begin{aligned}S^x_{i'j'}&=\phi(u,v)-\phi\left(u+s_x/(\lambda R),v\right)=\phi_{i'j'}-\phi_{i'+1,j'},\ i'=1,2,\cdots,m-1,\ j'=1,2,\cdots,n\\ S^y_{i'j'}&=\phi(u,v)-\phi\left(u,v+s_y/(\lambda R)\right)=\phi_{i'j'}-\phi_{i',j'+1},\ i'=1,2,\cdots,m,\ j'=1,\cdots,n-1,\end{aligned} \tag{12}$$

where $u=x_{i'}/(\lambda R), v=y_{j'}/(\lambda R)$.

Using the least square method[18], a recursive solution formula for the absolute phase can be derived:

$$\phi_{i'j'}=\frac{1}{4}\left(\phi_{i'+1,j'}+\phi_{i'-1,j'}+\phi_{i',j'+1}+\phi_{i',j'-1}+S^x_{i'j'}-S^x_{i'-1,j'}+S^y_{i'j'}-S^y_{i',j'-1}\right),\ i',j'=2,\cdots,m-1. \tag{13}$$

To eliminate phase unwrapping, replace equation (13) with equation (14) to get the target phase spectrum:

$$\phi_{i',j'} = \arg\left\{\frac{1}{4}\exp\left(\mathrm{i}\left(\phi_{i'+1,j'} + S^{x}_{i'j'}\right)\right) + \frac{1}{4}\exp\left(\mathrm{i}\left(\phi_{i'-1,j'} - S^{x}_{i'-1,j'}\right)\right) + \frac{1}{4}\exp\left(i\left(\phi_{i',j'+1} + S^{y}_{i'j'}\right)\right) + \frac{1}{4}\exp\left(i\left(\phi_{i',j'-1} - S^{y}_{i',j'-1}\right)\right)\right\}. \tag{14}$$

Using the amplitude and phase of the target, the target image can be reconstructed via inverse Fourier transform[19].

2.3 Constraint condition of the proposed imaging system

According to the SBI principle, when the laser wavelength and imaging distance are constant, the imaging resolution is determined by the size of the detector array. Since the detector array size of the proposed imaging system is the same as that of the traditional three-beam imaging system, the imaging resolution of the both imaging system is the same. When the size of the detector array is $D_x \times D_y$, the transverse imaging resolution is $1.43\lambda R / D_x$, and the longitudinal imaging resolution is $1.43\lambda R / D_y$ [15].

When the target size is $T_x \times T_y$, the laser detector spacing should satisfy the constraint condition $s_x \le \frac{2}{3}\lambda R / T_x$ and $s_y \le \frac{2}{3}\lambda R / T_y$. The number of lasers in emission array is $M \times N$, the detector spacings are $d_x = (M-1)s_x$ and $d_y = (N-1)s_y$. The transverse dimension and the longitudinal dimension of the receiving array are $m = \lfloor D_x / ((M-1)s_x) \rfloor$ and $n = \lfloor D_y / ((N-1)s_y) \rfloor$, respectively.

3. NUMERICAL SIMULATION

The Strehl ratios (SR) is used to evaluate reconstructed image quality, which is defined as follows [19]:

$$SR = \frac{\left|\iint O_a(x,y)O_b(x,y)dxdy\right|^2}{\iint O_a(x,y)O_a^*(x,y)dxdy \iint O_b(x,y)O_b^*(x,y)dxdy},$$

where $O_a(x,y)$ is the intensity distribution of reconstruction image without errors and $O_b(x,y)$ is the intensity distribution of reconstruction image with errors. "*" represents conjugate. The closer the Strehl ratios is to 1, the better the imaging quality.

The number of coherent laser beams is 9, the imaging distance is 1100km, the target size is 7.6×7.6m, the laser wavelength is 1064nm. The frequency of the 9 beams is 80MHz, 80MHz +10Hz, 80MHz+50Hz, 80MHz+120Hz, 80MHz+250Hz, 80MHz+270Hz, 80MHz+350Hz, 80MHz+410Hz, 80MHz+440Hz, and its layout is shown in Figure 2. The frequency differences of the beams are 0Hz, 10Hz, 50Hz, 120Hz, 250Hz, 270Hz, 350Hz, 410Hz, and 440Hz, respectively. The emission shear length s_x=0.1m, s_y=0.1m, the detector spacing d_x=0.2m, d_y=0.2m, and the number of detector elements in the receiving array is 43×43. The sampling frequency is 4000Hz and the number of sampling points is 12000.

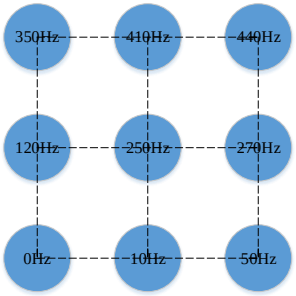

Figure 2. The frequency of laser beams (base frequency is 80MHz).

The parameters of the traditonal three-beam imaging system: the frequency of the three beams is 40MHz, 80MHz+100Hz, 80MHz+150Hz, respectively. The emission shear length s_x =0.1m, s_y =0.1m, the detector spacing d_x =0.1 m, d_y =0.1m, and the number of detector elements in the receiving array is 86×86. The sampling frequency is 4000Hz and the number of sampling points is 12000.

Two grayscale images are selected as targets, as shown in Figures 3 (a) (d). The reconstruction image of the two-dimensional spatial sparse reconstruction algorithm proposed in this paper is shown in Figures 3 (b) and 3(e), and the reconstruction image of the traditional three-beam reconstruction algorithm is shown in Figures 3 (c) and 3(f). All the reconstruction images are the result after an average of 40 times. According to the simulation results in Figure 3, after the number of detector elements is sparse by four times, the reconstructed image Strehl ratio of two-dimensional spatial sparse reconstructed algorithm is almost equal to that of traditional three-beam reconstructed algorithm. Thus, the two-dimensional spatial sparse reconstruction algorithm is effective and feasible.

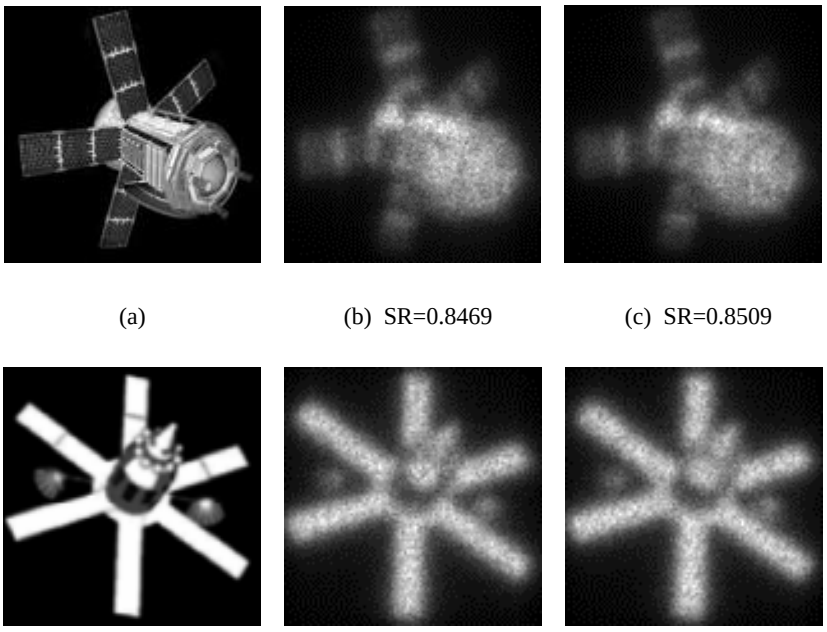

(a) (b) SR=0.8469 (c) SR=0.8509

(d) (e) SR=0.7996 (f) SR=0.7916

Figure 3. The reconstructed image and Strehl ratios: (a) (d) Origin target image; (b)(e) two-dimensional sparse reconstruction algorithm; (c)(f) traditional three-beam reconstruction algorithm.

In the following, the number of detector elements is sparse by nine times. The layout of coherent laser array is shown in Figure 4. The emission shear length s_x =0.1 m, s_y =0.1 m, the detector spacing d_x =0.3m, d_y =0.3m, and the number of detector elements in the receiving array is 29×29. The reconstruction images of the two-dimensional spatial sparse reconstruction algorithm is shown in Figures 5(a) and 5(b).

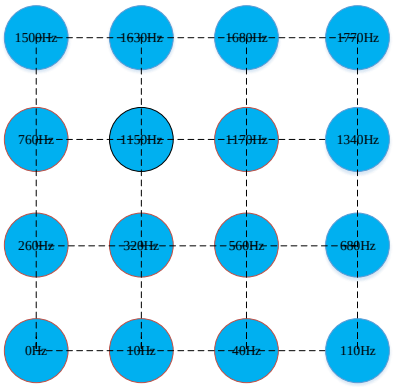

Figure 4. The frequency of laser beams (base frequency is 80MHz).

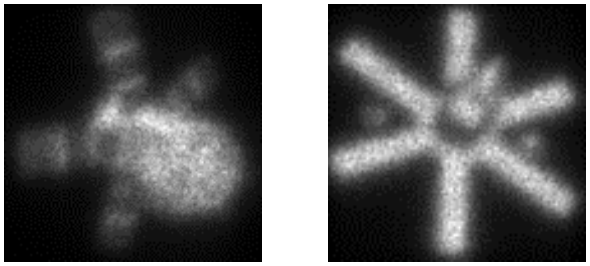

(a) SR=0.8456 (b) SR=0.7951

Figure 5. The reconstructed image and Strehl ratios of the two targets.

From figures 3(c) and 5(a), figures 3(f) and 5(b), it can be seen that the reconstructed image Strehl ratio of two-dimensional spatial sparse reconstruction algorithm is almost equal to that of traditional three-beam reconstruction algorithm when the number of detector elements is sparse by nine times. Therefore, the two-dimensional spatial sparse reconstruction algorithm is effective and feasible.

4. CONCLUSION

In order to overcome the problem that the number of detector elements in the SBI system is very large when imaing low-orbit moving targets, a sparse sampling method in the two-dimensional spatial domain for SBI receiving system is proposed. We investages a two-dimensional sparse sampling reconstruction algorithm, and gives a wavefront recovery method to reconstruct the target image. Numerical simulation results demonstrate that when the number of coherent lasers is $M \times N$, the target image can be reconstructed when the number of detector elements of the two-dimensional sparse sampling imaging system is $1/(M\text{-}1)/(N\text{-}1)$ of the traditional three-beam imaging system, and the image quality of the both system is nearly the same. The proposed sparse sampling method in the two-dimensional spatial domain is effective and feasible. It reduces the difficulty and cost of detector array development and can promote the engineering application of this technology.

ACKNOWLEDGMENTS

Project supported by the Natural Science Basic Research Program of Shaanxi (Program No. 2020JQ-438).

REFERENCES

[1] Tyson, R. K., Frazier, B. W., Principles of Adaptive Optics (5th Edition), CRC Press, Boca Raton, (2022).

[2] Luo, X. J., Liu, H., Zhang, Y., Chen, M. L., Lan, F. Y., “Review of ground-based optical imaging techniques for dim GEO objects,” Chin. Opt., 12(4), 753-766 (2019).
[3] Voelz, D. G., “Principles and applications of unconventional laser imaging,” Proc. SPIE, 2566, 74-79 (1995).
[4] Hutchin, R. A., “Sheared coherent interferometric photography: a technique for lensless imaging,” Proc. SPIE, 2029,161-168 (1993).
[5] Hutchin, R. A., Active imaging system and method, US, No.20120162631A1 (2012).
[6] Sica, L., “Sheared-beam imaging: an evaluation of its optical compensation of thick atmospheric turbulence,” Appl. Opt., 35(2):264-272 (1996).
[7] Lan, F. Y., Luo, X. J., Fan, X. W., Zhang, Y., Chen, M. L., Liu, H., Jia, H., “Effect of uplink atmospheric wavefront distortion on image quality of sheared-beam imaging,” Acta Phys. Sin., 67(20), 204201 (2018).
[8] Landesman, B. T., Kindilien, P., Pierson, R. E., Matson, C. L., Mosley, D., “Active imaging through cirrus clouds,” Opt. Express, 1(11), 312-323 (1997).
[9] Landesman, B. T., Olson, D. F., “Sheared beam imaging in the presence of space-time distortions,” Proc. SPIE, 2302, 14-25 (1994).
[10] Bush, Keith A., Barnard, Calvin C., Voelz, David G., “Simulations of atmospheric anisoplanatism effects on laser sheared beam imaging,” Proc. SPIE, 2828, 362-373 (1996).
[11] Chen, M. L., Luo, X. J., Zhang, Y., Lan, F. Y., Liu, H., Cao, B., Xia, A. L., “Sheared-beam imaging target reconstruction based on all-phase spectrum analysis,” Acta Phys. Sin., 66(2), 024203 (2017).
[12] Stahl, S. M., Kremer, R., Fairchild, P., Hughes, K., Spivey, B., Stagat, R., “Sheared-beam coherent image reconstruction,” Proc. SPIE, 2847, 150-158 (1996).
[13] Lan, F. Y., Luo, X. J., Chen, M. L., Zhang, Y., Liu, H., “Sheared-beam imaging of object with depth information,” Acta Phys. Sin., 66(20), 204202 (2017).
[14] Voelz, D. G., Gonglewski, J. D., and Idell P. S., “SCIP computer simulation and laboratory verification,” Proc. SPIE, 2029, 169-176 (1993).
[15] Chen, M. L., Liu, H., Zhang, Y., Luo, X. J., Ma, C. W., Yue, Z. L., Zhao, J., “Spatial domain sparse reconstruction algorithm of sheared beam imaging,” Acta Phys. Sin., 19, 194201 (2022).
[16] Atkinson, M. D., Santoro, N., Urrutia, J., “Integer sets with distinct sums and differences and carrier frequency assignments for nonlinear repeaters,” IEEE Trans. Commun., 34, 614-617 (1986).
[17] Goodman, J. W., Statistical Optics, J. Wiley, New York, pg. 495 (1985).
[18] Takajo, H. and Takahashi, T., “Least-squares phase estimation from the phase difference,” J. Opt. Soc. Am. A, 5(3), 416-425 (1988).
[19] Tyson, R. K., Principles and Applications of Fourier Optics, IOP Publishing, Bristol, UK (2014).